Regulatory T cells with superior immunosuppressive capacity emigrate from the inflamed colon to draining lymph nodes

Y Nakanishi[1,2,3], R Ikebuchi[1,2,4], T Chtanova[5,6], Y Kusumoto[2], H Okuyama[2], T Moriya[2], T Honda[7], K Kabashima[7], T Watanabe[8], Y Sakai[3] and M Tomura[1,2]

Foxp3$^+$ Regulatory T cells (Tregs) play a critical role in the maintenance of colon homeostasis. Here we utilized photoconvertible KikGR mice to track immune cells from the caecum and ascending (proximal) colon in the steady state and DSS-induced colitis. We found that Tregs from the proximal colon (colonic migratory Tregs) migrated exclusively to the distal part of mesenteric lymph nodes (dMLN) in an S1PR1-dependent process. In the steady state, colonic migratory CD25$^+$ Tregs expressed higher levels of CD103, ICOS, LAG3 and CTLA-4 in comparison with pre-existing LN Tregs. Intestinal inflammation led to accelerated Treg replacement in the colon, bidirectional Treg migration from the colon to dMLN and vice versa, as well as increases in Treg number, proliferation and expression of immunosuppressive molecules. This was especially apparent for CD25 very high Tregs induced in colitis. Furthermore, colonic migratory Tregs from the inflamed colon included more interleukin (IL)-10 producing cells, and demonstrated greater inhibition of T-cell proliferation in comparison with pre-existing LN Tregs. Thus, our results suggest that Tregs with superior immunosuppressive capacity are increased both in the colon and dMLN upon inflammation. These Tregs recirculate between the colon and dMLN, and are likely to contribute to the downregulation of intestinal inflammation.

Foxp3$^+$ Regulatory T cells (Tregs) inhibit immune cell function, and play critical roles in self-tolerance and maintenance of homeostasis.[1,2] Autoimmune symptoms including colitis are frequently observed in patients with immune dysregulation, polyendocrinopathy, enteropathy and in X-linked (IPEX) syndrome caused by a mutation in the *FOXP3* gene.[3] Similar symptoms were observed after Treg depletion in mice,[4] indicating a crucial role for Tregs in the maintenance of colon homeostasis. Changes in Treg number and the expression of immunosuppressive molecules are strongly associated with severity of inflammatory bowel disease (IBD) including Crohn's disease and ulcerative colitis. Notably, while Treg numbers are elevated in activated mucosal IBD regions, they decrease after amelioration of inflammation in IBD patients.[5,6] Furthermore, Tregs mediate tolerance and suppress effector T (Th17 and Th1) cell function exacerbated in colitis, thereby facilitating a cure of colitis.[7,8] Treg-derived cytokine IL-10 is critical for the maintenance of colon homeostasis[9] and ICOS$^+$ Tregs often produce IL-10 (ref. 10). In addition, immunosuppressive surface molecules CTLA-4, LAG-3, PD-1, and Galectin-9 inhibit T cell activation *via* an IL-10 independent pathway.[11–14]

Commensal microbiota including Clostridia strains and *Bacteroides fragilis* facilitate differentiation and maintenance of colonic Treg functions, including microbiota-induced expression of ICOS, CTLA-4, and IL-10 (refs 15,16). Consistent with the enrichment of Treg-inducible microbiota in the proximal colon,[17] Tregs are abundant at this site in healthy humans.[18] Furthermore, colonization by Clostridia strains induces Tregs and resistance to dextran sulfate sodium (DSS)-induced colitis

[1]Center for Innovation in Immunoregulative Technology and Therapeutics, Graduate School of Medicine, Kyoto University, Kyoto, Japan. [2]Laboratory of Immunology, Faculty of Pharmacy, Osaka Ohtani University, Tondabayashi, Osaka, Japan. [3]Department of Surgery, Graduate School of Medicine, Kyoto University, Kyoto, Japan. [4]Research Fellow of Japan Society for the Promotion of Science, Japan. [5]Immunology Division, Garvan Institute of Medical Research, Darlinghurst, NSW, Australia. [6]St Vincent's Clinical School, Faculty of Medicine, University of New South Wales Sydney, Darlinghurst, New South Wales, Australia. [7]Department of Dermatology, Kyoto University Graduate School of Medicine, Kyoto, Japan and [8]The Tazuke-Kofukai Medical Research Institute/Kitano Hospital, Kita-ku, Osaka, Japan. Correspondence: M Tomura (michio.tomura@gmail.com)

Received 28 December 2016; accepted 3 June 2017; published online 2 August 2017. doi:10.1038/mi.2017.64

in mice.[19] These results suggest that Tregs induced in the caecum and ascending colon are involved in systemic immune responses. To unravel the role of colonic Tregs in local and systemic immune responses, Treg migration pathways from the caecum and ascending colon need to be defined both in the steady state and during inflammatory disease.

Photoconvertible fluorescent proteins Kaede, and Kikume Green Red (KikGR) can be irreversibly converted from green to red upon exposure to violet light.[20,21] We previously established an *in vivo* cell tracking system, which utilizes Kaede transgenic and KikGR knock-in mice to trace cell migration from a photoconverted organ to distal anatomical sites.[22,23] In an earlier study, photoconversion of the descending colon in Kaede transgenic mice suggested involvement of colon-derived effector T cells in the onset of systemic autoimmune diseases.[24] Furthermore, we previously reported that skin immune response enhances bidirectional migration of $CD4^+$, and especially $Foxp3^+$, T cells between cutaneous draining lymph node (LN) and inflamed skin. Tregs that emigrated from the inflamed skin to the draining LN included a novel Treg subset with superior immunosuppressive properties including high levels of TGF-β, CTLA-4, and IL-10, that may contribute to remission of skin contact hypersensitivity.[25] Thus, we examined whether colonic inflammation alters cellular movement between the colon and draining LN and induces superior immunosuppressive Tregs that can cure colitis.

In this study, we provide insights into the mechanisms of Treg migration between the colon and secondary lymphoid organs and the role of these Tregs in intestinal homeostasis. We utilized KikGR mice to label cells in the proximal colon and investigated migration and function of colonic T cells in the steady state and in a typical IBD model, DSS-induced colitis. We found that Tregs with superior immunosuppressive potential migrated from the caecum and ascending colon exclusively to the distal part of mesenteric LN (dMLN). Colon inflammation induced accelerated Treg turnover and proliferation in the colon and dMLN, and bidirectional movement between colon and dMLN. Furthermore, Tregs emigrating from the inflamed colon to dMLN were better at inhibiting T-cell proliferation and expressed higher levels of immunosuppressive molecules, such as IL-10, compared to Tregs in dMLN.

RESULTS

Identification of the draining sites for the caecum and ascending colon

Murine MLN consists of several nodules and lymphatic fluid from discrete portions of the intestinal tract drains to separate lymph nodes.[26] Furthermore, a recent study characterized immune cell migration from the intestinal tract to specific MLN regions.[27] However, the precise draining sites for the caecum and colon remain to be defined. To investigate the anatomical

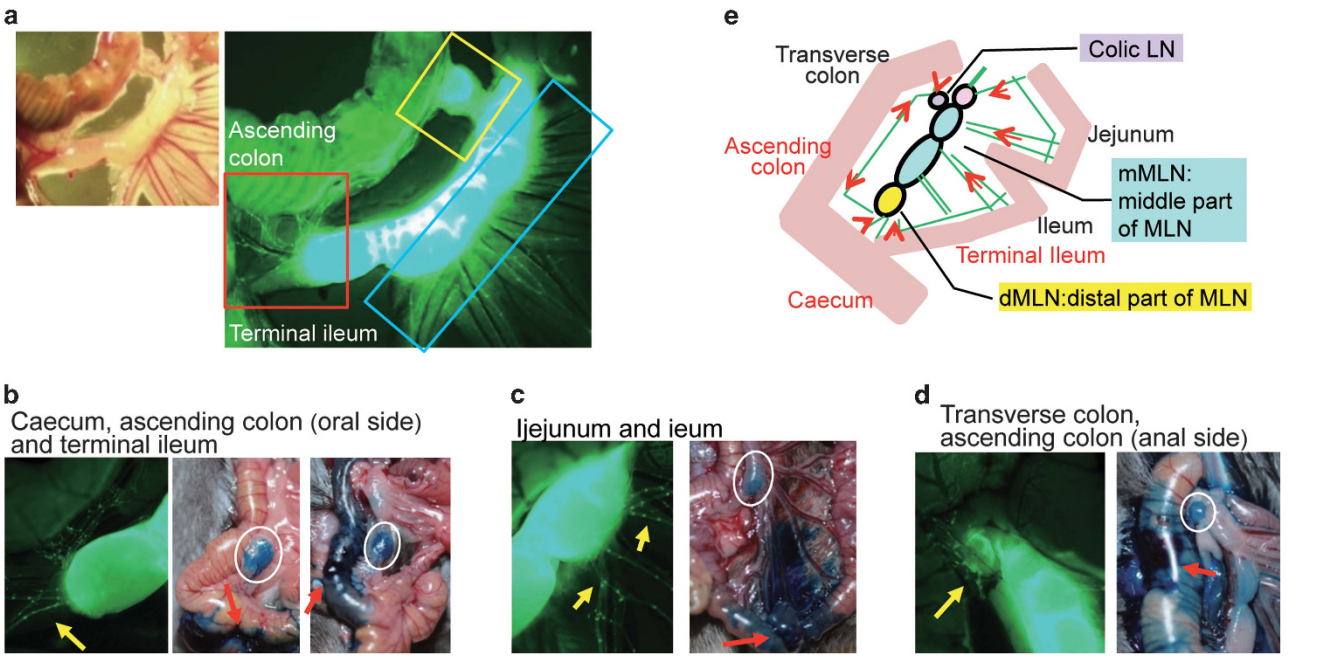

Figure 1 Afferent lymph vessels from the caecum, ascending colon, and small intestine are anatomically linked to distinct regions of mouse mesenteric lymph nodes. Mesentery of Prox1-GFP mice were observed with a fluorescence stereoscopic microscope. (**a**) Bright field (small image), fluorescence channel (large image). Afferent lymph vessels from the terminal ileum, caecum, and ascending colon linked to distal part of mesenteric lymph nodes (MLN; red box), vessels from the jejunum and ileum linked to middle and proximal part of MLN (blue box), and vessels from the transverse colon connected to colic LN (yellow box), (**b**–**d**) Fluorescence (left panel) and lymphography (center and right panels) images are shown. Patent blue was injected to caecum (center panel) and ascending colon (right panel) (**b**), ileum (**c**), and transverse colon (**d**). Yellow arrows indicate afferent lymph vessels. Red arrows indicate injection sites of patent blue dye. White circles indicate patent blue-stained regions in MLN. Data are representative of at least three independent experiments. (**e**) Diagram of lymph drainage and cell migration data from gut to mesenteric lymph nodes in mice. Distal part of MLN (dMLN) is indicated in yellow. Middle part of MLN (mMLN) is indicated in pale blue. Proximal part of MLN is indicated in pink. Colic LN is indicated in purple.

features of murine mesentery in greater detail, we used Prox1-GFP mice (which express GFP in lymphatic vessels under the control of Prox1, a master control gene of lymphoid tissue differentiation) to visualize lymphatic vessels.[28] Afferent lymphatic vessels of the terminal ileum, caecum and ascending colon were connected to the dMLN (**Figure 1a** red box and **Figure 1b**). On the other hand, afferent lymph vessels of the jejunum and ileum were connected to the middle and proximal part of the MLN (mMLN; **Figure 1a** blue box and **Figure 1c**), and those of the transverse colon were connected to the colic lymph node (**Figure 1a** yellow box and **Figure 1d**).[29] Lymphography showed that the corresponding regions of the MLN were colored after dye injection at specific sites of the intestinal tract (**Figures 1b–d**). We noted that individual afferent vessels from different regions of intestinal tract lay along the intestinal tract, and coalesced into bundles and reached distinct MLN regions. Anatomical illustration of the gut, afferent lymph vessels and MLN is shown in **Figure 1e**.

We next set out to track immune cell migration from the caecum and ascending colon (hereafter called proximal colon) using KikGR/Foxp3$^{hCD2/hCD52}$ mice. These mice express photoconvertible protein KikGR, which allows us to label cells by exposing them to violet light and track them *in vivo*, whereas Foxp3$^+$ Tregs in these mice can be identified by the expression of human CD2 (hCD2) (ref. 30). To label cells in specific areas of the colon, the caecum was surgically exposed through a small incision in the midline just below the costal margin and exposed to violet light for 2 min. Then, the caecum was returned to the abdomen and the ascending colon was exposed to light. Upon exposure violet light, cells in the photoconverted region of the colon in KikGR/Foxp3$^{hCD2/hCD52}$ mice were converted from green (KikGR-Green) to red (KikGR-Red; **Supplementary Figure S1 online**). Flow cytometric analysis showed that immediately after photoconversion of the proximal colon (as shown in **Figure 2a**), almost 80% of cells in the exposure site expressed KikGR-Red, indicating that photoconversion successfully labeled the majority of the colon-infiltrating cells (**Figure 2b**). In contrast, no photoconverted cells were detected in dMLN, mMLN, and cutaneous lymph nodes (CLNs) immediately after photoconversion indicating that photoconversion was restricted to the target tissue (**Supplementary Figure S2**). However, 6 h after photoconversion, while a large proportion of photoconverted cells remained in the colon, the majority of migratory photoconverted cells were detected in dMLN rather than mMLN (**Figure 2c** and **Supplementary Figure S3**). Furthermore, using *in vivo* microscopy we observed photoconverted cells migrating through the GFP$^+$ afferent lymph vessels in real time following photoconversion of the proximal colon in Prox1-GFP chimeric mice containing KikGR/Foxp3$^{hCD2/hCD52}$ bone marrow (**Supplementary Video S1**).

In order to confirm the region of draining MLN that cells migrating from the proximal colon and small intestine accumulate in, we monitored migratory dendritic cells (DCs) since these cells do not readily egress draining LN.[23] Following photoconversion of the proximal colon as in **Figure 2a** or the jejunum and ileum (excluding the terminal ileum) as in **Figure 2d**, photoconverted DCs were detected in CD11c$^+$MHC Class II^{high} migratory DC population in mMLN or dMLN (**Supplementary Figure S4**). In addition, after photoconversion of the proximal colon, photoconverted mucosae-derived CD103$^+$ DCs[31] were detected in dMLN, but not in mMLN and CLNs

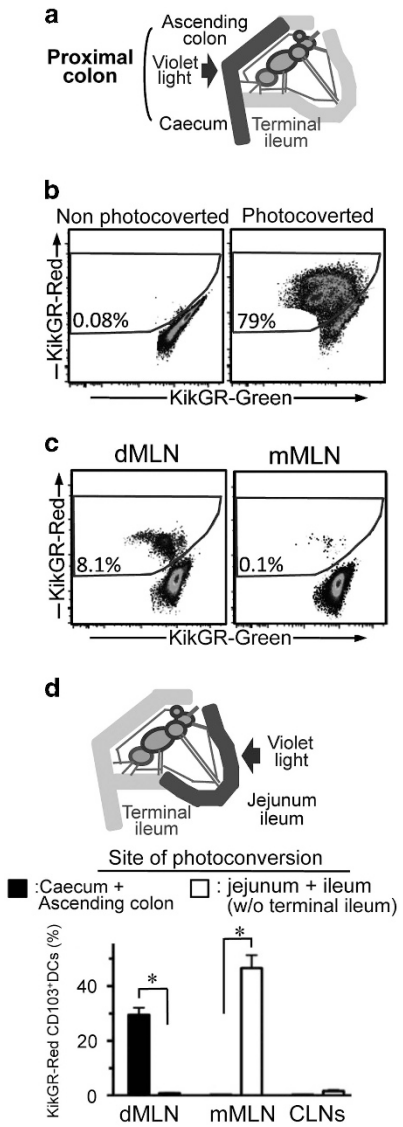

Figure 2 Immune cells in the caecum and ascending colon migrate to exclusively distal part of MLN. (**a**) Caecum and ascending colon (proximal colon) of KikGR/Foxp3$^{hCD2/hCD52}$ mice were photoconverted as indicated in the diagram. (**b**) Expression of KikGR-Green and KikGR-Red by cells isolated from the proximal colon of KikGR/Foxp3$^{hCD2/hCD52}$ mice before and after photoconversion. (**c**) KikGR-Green and KikGR-Red expression by cells isolated from dMLN and mMLN 6 h after photoconversion of the proximal colon of KikGR/Foxp3$^{hCD2/hCD52}$ mice. (**d**) Proportions of photoconverted cells among CD103$^+$ DCs in dMLN, mMLN, and CLNs (pool of cervical and axillary LNs), 24 h after photoconversion of the proximal colon or small intestine (except for terminal ileum). Flow cytometry gating strategy for CD103$^+$ DCs is shown in **Supplementary Figure S4a**. Flow cytometry data in **b** and **c** are representative of at least two independent experiments with three mice per group; values in the plots indicate the percentage of the parent population. Data in (**d**) is represented as means ± SEM (**d**; $n = 5$). Statistical comparisons were performed using Mann–Whitney's *U*-test (*$P < 0.05$).

(**Supplementary Figure S5a** and **Figure 2d**). In contrast, following photoconversion of the jejunum and ileum (excluding the terminal ileum), migratory photoconverted DCs were detected in mMLN, but not in dMLN (**Figure 2d**). Thus, intestinal immune cells migrate only to specific MLN regions in mice, and cells from both the proximal colon and terminal ileum migrate to dMLN.

Tregs in the caecum and ascending colon initially migrate to dMLN

Tregs in the colon and MLN are critical for maintenance of colonic immune homeostasis.[32] We previously reported that in the steady state Tregs in peripheral tissues such as skin continuously migrate to draining LN.[25] To investigate Treg migration from the proximal colon, we subdivided T cells in KikGR/Foxp3$^{hCD2/hCD52}$ mice into 3 subsets; CD8$^+$ T cells, CD4$^+$Foxp3$^-$ T cells (Tconvs), and CD4$^+$Foxp3$^+$ T cell (Tregs; **Supplementary Figure S5b and c**). After photoconversion of the proximal colon, almost 80% of cells were photoconverted in each T cell subset (**Figure 3a**). Time course analysis revealed that photoconverted cells first appeared in dMLN. The proportions and numbers of photoconverted cells in all T-cell subsets in dMLN were highest at 6 h after photoconversion and gradually decreased by 96 h (**Figure 3b** and **Supplementary Figure S6**). The number of photoconverted T cells in the CLNs, spleen, and in mMLN adjacent to dMLN increased more slowly and plateaued by 24 h after colon photoconversion for mMLN, and 48 h for CLNs and spleen, respectively (**Figure 3b**).

Colonic migratory Tregs egress the colon in an S1P-dependent manner

Although the molecular mechanism of lymphocyte homing to the colon has been extensively studied, the mechanism of immune egress from the colon is yet to be identified. Sphingosine-1-phosphate receptor 1 (S1PR1) is used for T cell emigration from LN.[33,34] Thus, we examined whether colonic T cells use S1P-S1PR1 pathway to egress the colon. Thirty minutes prior to photoconversion of the proximal colon we treated mice with FTY720, an S1PR1 agonist, which blocks the S1P-S1PR1 pathway by downregulating S1PR1, and prevents T-cell egress from tissues.[33–35] Flow cytometric analysis showed that 24 h after FTY720 administration, the proportion of photoconverted cells in all T-cell subsets in the colons of FTY720-treated mice was significantly higher than in control mice (**Figure 3c**). We also detected a concomitant decrease in the proportion of photoconverted T cells in dMLN of FTY720-treated mice compared to control animals. Furthermore, colons of FTY720-treated mice contained nearly the same proportion of photoconverted cells after 24 h (~80%) as recently photoconverted colons (**Figure 3a**) indicating that the majority of colonic migratory T cells were retained following treatment and T regs, Tconvs and CD8$^+$ T-cell egress of the colon is S1P-dependent.

Colonic migratory Tregs in dMLN possess superior immunosuppressive potential

Next we conducted a detailed analysis of colonic migratory Tregs in draining LN. We previously demonstrated that skin migratory Tregs in draining LN are mainly CD44^{high} (refs. 25,36). Twenty-four hours after photoconversion of the proximal colon, similar frequencies of CD62L^{low}CD44^{high} effector memory cells were detected among photoconverted and non-photoconverted Treg populations in dMLN (**Figure 4a**). Photoconverted Tregs expressed modestly higher levels of immunosuppressive molecules CD103, ICOS, LAG3, PD-1, and CTLA-4 compared to non-photoconverted Tregs in dMLN (**Figure 4b** and **Supplementary Figure S7b**). Cell surface molecule CD25 has previously been used to identify Tregs. Furthermore, Tregs can be subdivided into CD25$^+$ and CD25$^{lo/-}$ subsets with distinct features.[28] Therefore, we compared photoconverted and non-photoconverted CD25$^+$ and CD25$^{lo/-}$ Tregs subsets in dMLN (**Figure 4c**). Interestingly, CD25$^+$ Tregs expressed higher levels of CD103, ICOS, LAG3, and CTLA-4 compared to

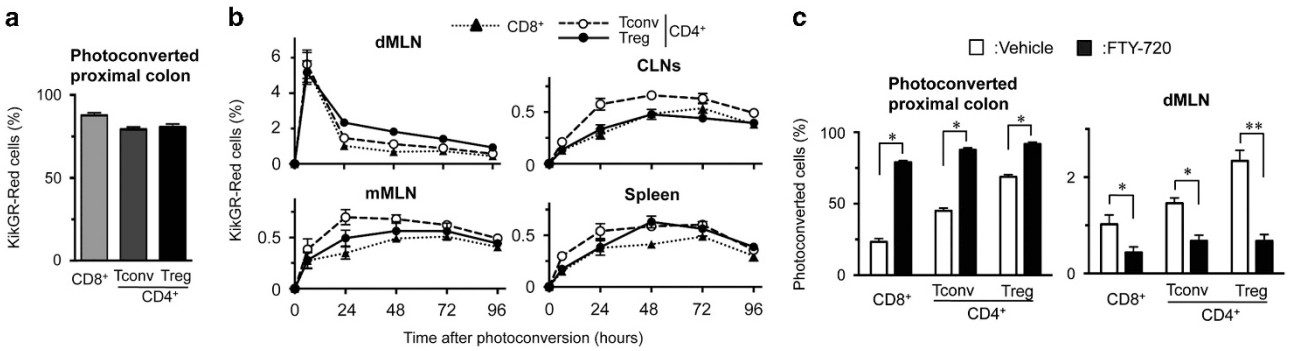

Figure 3 Tregs egress the colon in an S1PR1-dependent manner and migrate to dMLN. Proximal colons of KikGR/Foxp3$^{hCD2/hCD52}$ mice were photoconverted and flow cytometric analysis was performed. Flow cytometry gating strategy for CD8$^+$ T cells, Tconvs, and Tregs is shown in **Supplementary Figure S2b and c**. (**a**) The proportions of photoconverted cells in each T-cell subset at the site of photoconversion immediately after photoconversion. (**b**) The proportions of photoconverted cells in each T-cell subset in dMLN, mMLN, CLNs (pooled axillary and cervical lymph nodes), and spleen at indicated time points following photoconversion ($n = 5$–6). (**c**) FTY720 or vehicle was administered 30 min prior to photoconversion of the proximal colon of KikGR/Foxp3$^{hCD2/hCD52}$ mice and flow cytometric analysis was performed 24 h later. Proportions of photoconverted cells in each subset in the proximal colon (left), and dMLN (right) are shown. Data are representative of at least two independent experiments with three mice per group. Data in graphs represent means ± s.e.m. ($n = 3$–5). Statistical comparisons were performed using Mann–Whitney's *U*-test (**$P < 0.01$, *$P < 0.05$).

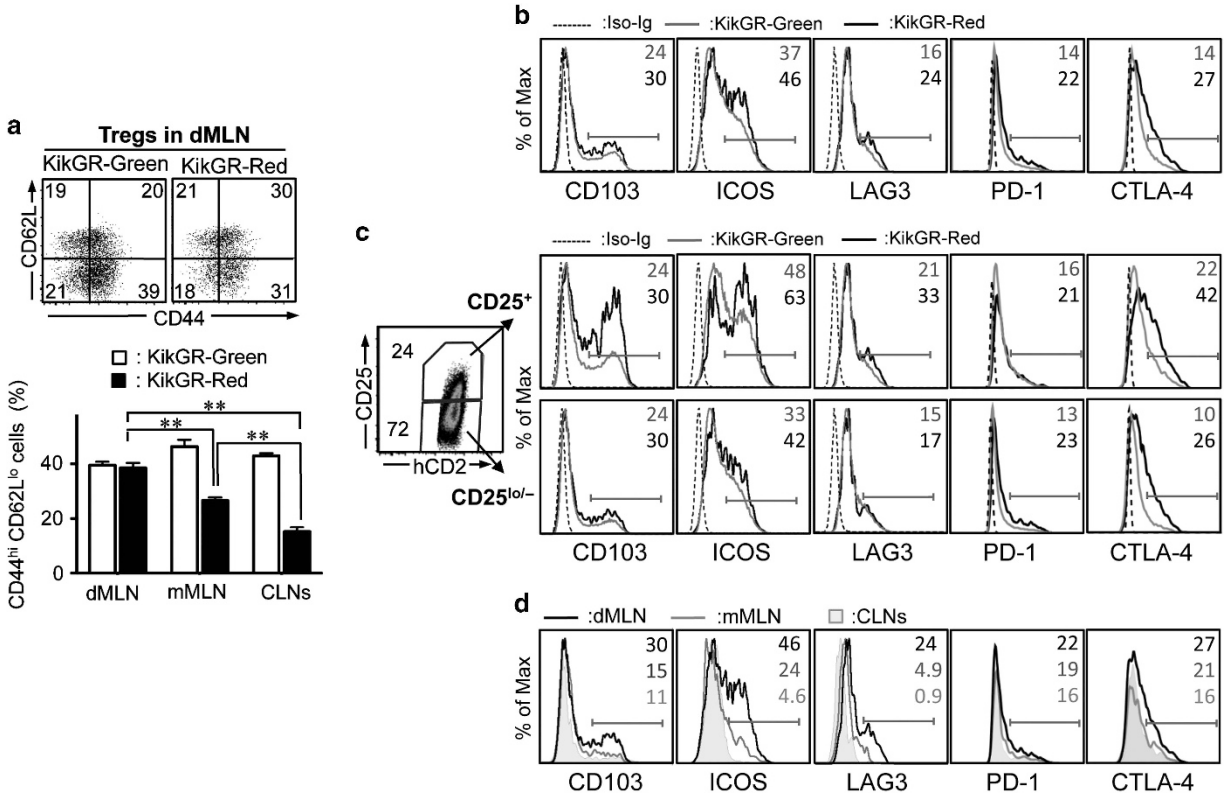

Figure 4 Colonic migratory Tregs in dMLN express higher levels of immunosuppressive molecules. (**a**) Proximal colons of KikGR/Foxp3$^{hCD2/hCD52}$ mice were photoconverted and flow cytometric analysis was performed 24 h following photoconversion. Proportions of CD44^{high} CD62L^{low} cell out of colonic migratory photoconverted Tregs (red) and non-photoconverted Tregs (green) in dMLN, mMLN, and CLNs. Data in graphs are represented as means ± SEM ($n=3$). Statistical comparisons were performed using Mann–Whitney's *U*-test (**$P<0.01$). (**b**) CD103, ICOS, LAG3, PD-1, and CTLA-4 expression in non-photoconverted LN Tregs and colonic migratory photoconverted Tregs in dMLN ($n=4$–6). (**c**) Flow cytometry gating strategy for CD25$^+$ and CD25$^{lo/-}$ Tregs in dMLN, and CD103, ICOS, LAG3, PD-1, and CTLA-4 expression in photoconverted and non-photoconverted CD25$^+$ and CD25$^{lo/-}$ Treg subsets ($n=4$–6). (**d**) Colonic migratory photoconverted Tregs in dMLN, mMLN, and CLNs ($n=4$–5). Flow cytometry data are representative of at least three independent experiments; values in the plots indicate the percentage of the parent population.

CD25$^{lo/-}$ Tregs in both photoconverted and non-photoconverted subsets, indicative of a superior immunosuppressive potential (**Figure 4c**). Thus, CD25$^+$ Tregs, particularly colonic migratory Tregs are likely to play an important role in the maintenance of immune homeostasis in the steady state in comparison to CD25$^{lo/-}$ Treg subsets. Interestingly, photoconverted colonic migratory Tconvs, but not CD8$^+$ T cells also expressed higher levels of CD103, ICOS, and LAG3 compared to non-photoconverted subsets in dMLN (**Supplementary Figure S7b** and **c**) indicating that this phenotype was not restricted to the Treg population. In addition, we found that both neuropilin-1 (Nrp-1)$^-$ peripherally induced Tregs (pTregs) and Nrp-1$^+$ thymus-derived Tregs (tTregs)[14,37] migrated from colon to dMLN. The proportion of pTregs among photoconverted Tregs was modestly reduced compared to non-photoconverted Tregs in CD25$^{lo/-}$ Treg subsets (**Supplementary Figure S7a** and **b**).

Notably, the proportion of CD62L^{low}CD44^{high} effector memory Tregs in dMLN was higher than in mMLN and CLNs (**Figure 4a**). We previously reported that CD44^{high} memory T cells express higher levels of CD69 and are retained in lymph nodes for an extended period of time.[34] Thus, these results suggest that colonic migratory Tregs with immunosuppressive function are retained in dMLN for longer than in the other LNs.

Colitis causes an increase in Treg number and proliferation in the colon and dMLN

In IBD patients, Tregs are increased in both the colon and MLN.[5,38] In addition, we noted that in the steady state colonic migratory Tregs in dMLN had a more immunosuppressive phenotype than total LN Tregs (**Figure 4**). To assess the role of these cells during inflammatory responses we examined changes in cellular dynamics and phenotype of colonic migratory Tregs in colitis. DSS-induced colitis was elicited by giving mice 3% DSS in drinking water for 7 days; control mice received regular drinking water (**Figure 5a**). Body weight loss and decrease in colon length correlated with colitis severity and peaked around day 9, then gradually recovered (**Figure 5a**, **Supplementary Figure S8a** and **b**). While all T cell subsets increased after day 6 in dMLN, (but not in mMLN), only Tregs and not Tconvs and CD8$^+$ T cell numbers increased in the colon (**Figure 5b** and **Supplementary Figure S8c**). These results reinforce the idea that dMLN rather than mMLN is the site for colonic immune response.

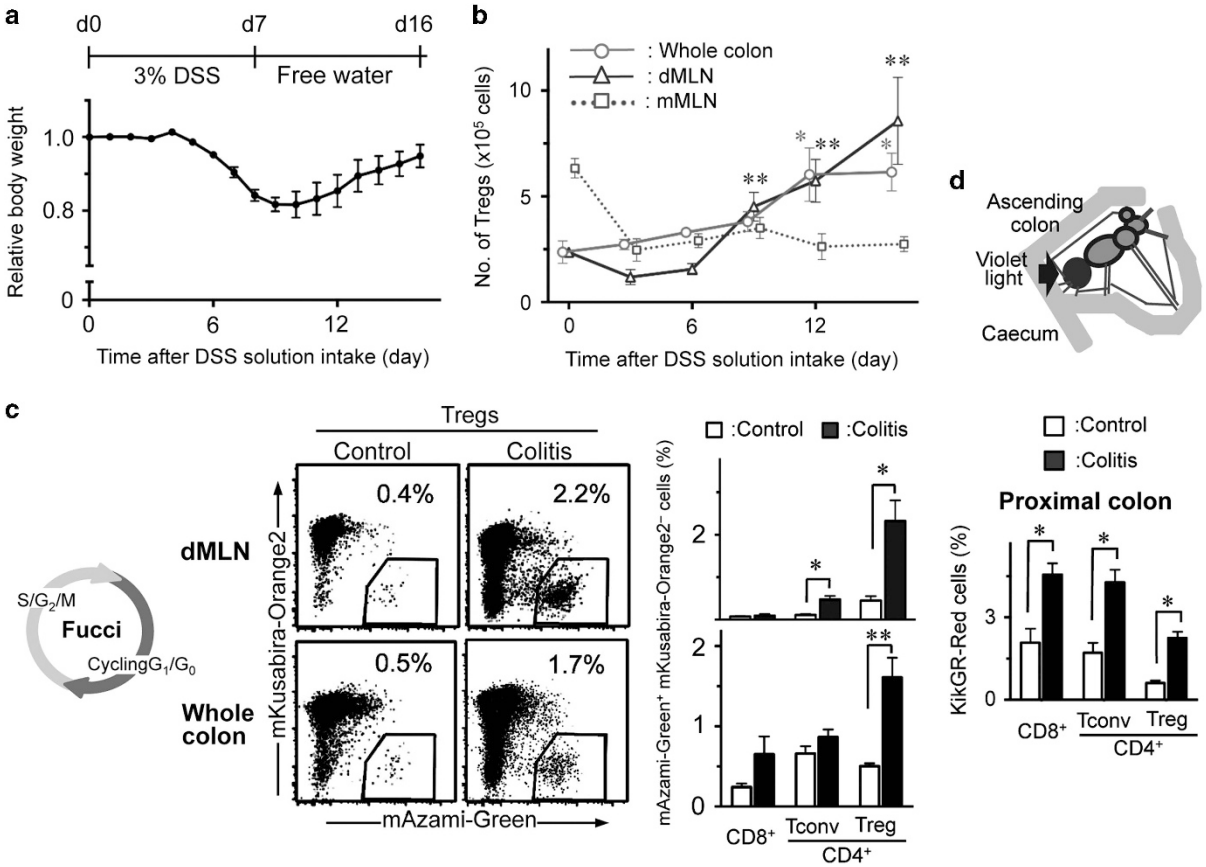

Figure 5 Colitis leads to increases in Treg number and proliferation in the colon and dMLN. Timeline for DSS-induced colitis is shown. Mice were given 3% DSS in drinking water for 7 days, then water alone. Relative body weight (**a**), and Treg number in the whole colon, dMLN, and mMLN in Foxp3$^{hCD2/hCD52}$ mice following induction of colitis (**b**). These data are representative of at least 2-3 independent experiments. (**c**) Proportions of mAzami-Green^{+} mKusabira-Orange2^{-} cells out of CD8^{+}, Tconv, and Treg subsets in dMLN and whole colon in DSS-treated and control Fucci-Tg/Foxp3$^{hCD2/hCD52}$ mice on day12 (Colitis). (**d**) dMLN of KikGR/Foxp3$^{hCD2/hCD52}$ mice with DSS-induced colitis and control mice were photoconverted on day12 (Colitis) and flow cytometric analysis was performed 24 h later. Flow cytometry data are representative of at least three independent experiments; values in the plots indicate the percentage of the parent population. Data in graphs is represented as means ± s.e.m. ($n = 5$–6). Statistical comparisons between day 0 and indicated day in each group were performed using Mann–Whitney's *U*-test (**$P < 0.01$, *$P < 0.05$).

We selected day 12 for the analysis of cellular movement, phenotype, and immunosuppressive capacity of colonic migratory Tregs in the recovery phase of colitis, since at this time we observed body weight recovery and increases in all T cell subsets in dMLN (**Figure 5a, b** and **Supplementary Figure S8**). To identify the sites of Treg proliferation we utilized Fucci-Tg/Foxp3$^{hCD2/hCD52}$ mice where cells exhibit red fluorescence during quiescent G_0 and cycling G_1 phase (due to fusion of mKusabira-Orange2 to hCdt1) and green fluorescence in S/G_2/M (fusion of mAzami-Green to hGeminin).[39] In comparison to steady-state controls, the proportion of Tregs in S/G_2/M phase (as well Tconvs but not CD8^{+} T cells) was drastically increased in dMLN of animals with colitis. Unexpectedly, Tregs in S/G_2/M phase were also increased in the colon (**Figure 5c**). These results show that colonic inflammation induces Treg proliferation not only in dMLN, but also in the colon.

Next, we examined Treg migration from dMLN to the colon during colitis. In this case, dMLN was photoconverted and cells in the colon were analyzed 24 h later (**Figure 5d**). Compared to the steady state, dMLN-egressing photoconverted T cells in the proximal colons of animals with colitis were significantly increased: 2.3 fold for CD8^{+} cells, 2.8 fold for Tconvs, and 3.1 fold for Tregs. Thus, T cell, and especially Treg, migration from dMLN to the colon was enhanced during recovery phase of colitis.

Colitis increases Treg turnover in the colon and emigration from the colon to dMLN

To explore Treg migration from the proximal colon, we photoconverted the proximal colon of animals with DSS-induced colitis and control mice on day 12. Similar to the steady state, we could photoconvert ~80% of cells in the proximal colon of mice with colitis (**Figure 6** left panel). Twenty-four hours after photoconversion of the proximal colons in control mice, the majority (85%) of photoconverted Tregs remained in the colon compared to only 54% of Tconvs. Thus, only 15% of Tregs were replaced in the proximal colon within 24 h in contrast to 46% of Tconvs replaced within the same time interval. Therefore, in steady state Tregs are preferentially retained in the colon. In contrast, photoconverted Treg

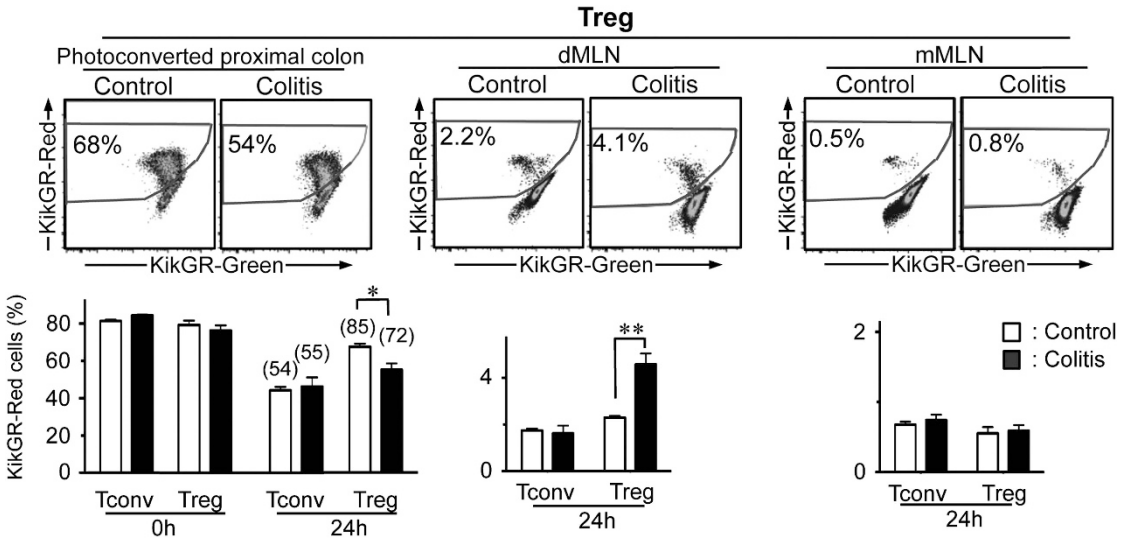

Figure 6 Colitis increases Treg turnover in the colon and Treg migration from the colon to dMLN. Proximal colons of DSS-treated and control of KikGR/Foxp3$^{hCD2/hCD52}$ mice (Colitis) were photoconverted on day 12 and flow cytometric analysis was performed immediately after photoconversion and 24 h later. The proportions of photoconverted Tregs at the site of photoconversion (proximal colon) (left panel), dMLN (middle panel), and mMLN (right panel) are shown. These flow cytometry data are representative of at least three independent experiments; values in flow cytometry plots indicate the percentage of the parent population, values in parenthesis in bar graph indicate the percentage of photoconverted cells after 24 h out of photoconverted cells at time 0. Data in bar graphs represent means ± s.e.m. ($n = 5$–8). Statistical comparisons were performed using Mann–Whitney's *U*-test (**$P < 0.01$, *$P < 0.05$).

frequency was reduced to 72% within 24 h of photoconversion of proximal colon in animals with colitis, indicating a 1.9-fold increase in Treg turnover in the inflamed colon compared to the steady state. This increase was specific to Tregs as turnover of Tconvs (**Figure 6** left panel) and CD8$^+$ T cells (data not shown) remained unchanged. Concomitant with increased Treg turnover within the inflamed colon, we noted an increase in both frequency and number of photoconverted Tregs in dMLN (**Figure 6** middle panel and **Supplementary Figure S9**) but not in mMLN and CLNs (**Figure 6** right panel and data not shown). Furthermore, the numbers of both non-photoconverted and photoconverted CD103$^+$ and CD103$^-$ DCs increased in dLN in colitis (**Supplementary Figure S10**). Taken together, the results in **Figures 5** and **6** suggest that inflammatory immune response increased Treg turnover within the colon and accelerated cellular movement from the colon to dMLN as well as from dMLN to colon.

Colitis induces CD25^{++} Treg expansion in the colon and draining LN, accelerated turnover and migration from the colon to draining LN

We previously reported that Tregs expressing exceptionally high levels of CD25 (CD25^{++} Tregs) migrate from inflamed skin to the draining LN and display a superior immunosuppressive capacity in skin immune responses.[25] In the present study, we analyzed whether CD25^{++} Tregs existed in colitis. CD25^{++} Tregs were detected both in the colon and dMLN, but not in mMLN and CLNs 12 days after induction of colitis (**Figure 7a** and data not shown). Thus, similarly to immune responses in inflamed skin, CD25^{++} Tregs are generated during colonic inflammatory response.

While proportions of CD25^{++} Tregs in the colon increased constantly after the DSS administration, those in dMLN started to increase only during the recovery phase of colitis, peaked on day 12 and then gradually decreased (**Figure 7b**). In addition, analysis of cell cycle progression in Fucci-Tg/Foxp3$^{hCD2/hCD52}$ mice revealed that a much greater proportion of CD25^{++} Tregs proliferated compared to CD25$^{+/-}$ Tregs both in the dMLN and colon (**Figure 7c**). In particular, a large proportion (18% of cells in S/G_2/M phase) of CD25^{++} Tregs in dMLN proliferated (**Figure 7c**). These results indicate that dMLN is the main site of CD25^{++} Treg proliferation, but some CD25^{++} Tregs also proliferate in the inflamed colon during colitis.

Next, we photoconverted dMLN as in **Figure 5d**, and analyzed Treg migration from dLN to the colon during inflammation. Twenty-four hours after photoconversion, both photoconverted CD25$^{+/-}$ and CD25^{++} Tregs could be detected in the proximal colon (**Figure 7d**). Finally, we photoconverted the proximal colon and analyzed cell migration from the proximal colon to the draining LN. Twenty-four hours following photoconversion, the proportion of photoconverted CD25^{++} Tregs remaining in the colon was lower compared to CD25$^{+/-}$ Tregs, however, more photoconverted CD25^{++} Tregs were found in dMLN (**Figure 7e**), indicating that CD25^{++} Treg turnover in the inflamed colon and their migration from the inflamed colon to the draining LN were faster than those of CD25$^{+/-}$ Tregs.

Colonic migratory Tregs in draining LN display immunosuppressive phenotype in colitis

Next we determined the phenotype of Tregs in colitis. ICOS, LAG3, PD-1, and CTLA-4 expression in Tregs in draining LN was increased in colitis compared to that in untreated mice (**Figures 4b , 8b**, **Supplementary Figure S7** and **S12**). Then, we subdivided Tregs into CD25$^{+/-}$and CD25^{++} subsets. ICOS,

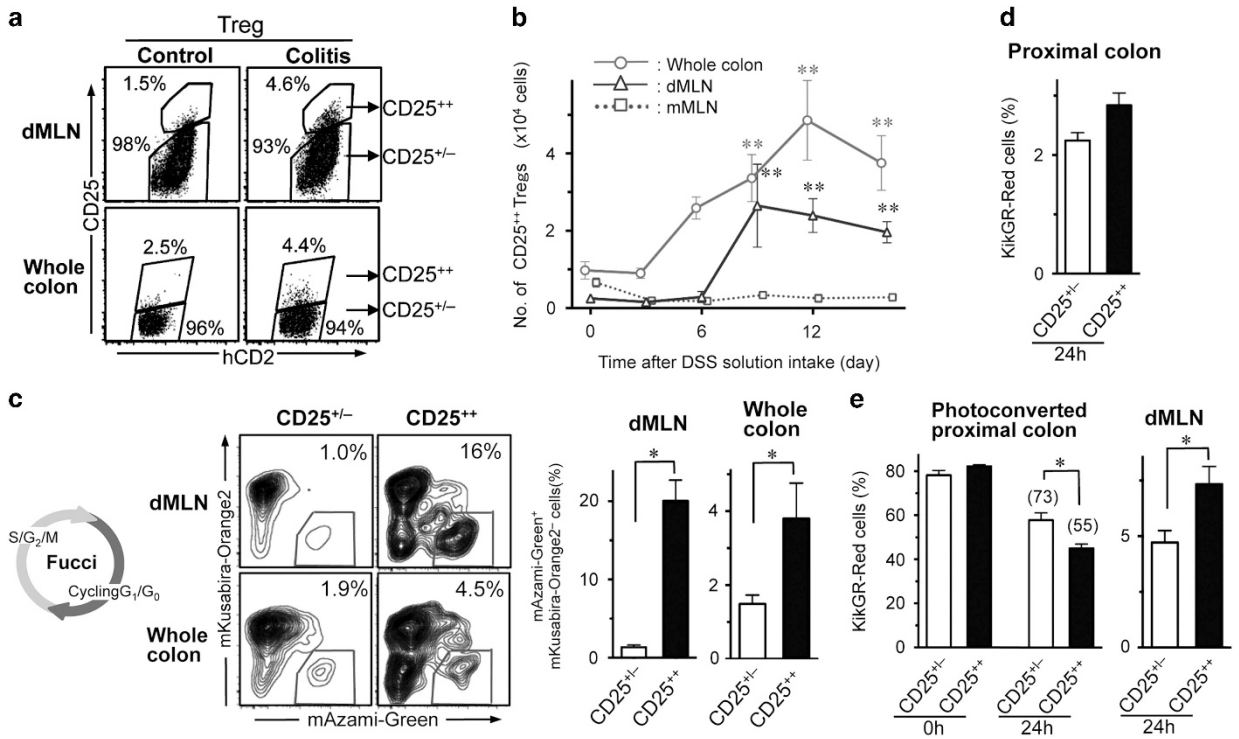

Figure 7 Highly proliferative and motile CD25^{++} Tregs are induced in colitis. (**a**) Flow cytometry gating strategy for CD25^{++} and CD25$^{+/-}$ Treg subsets in dMLN and whole colon. (**b**) Time course of CD25^{++} Treg cell number in the whole colon, dMLN, and mMLN following induction of DSS-induced colitis. (**c**) The proportions of mAzami-Green^{+} mKusabira-Orange2^{-} cells in CD25$^{+/-}$ and CD25^{++} Tregs in the dMLN and whole colon in DSS-treated and control Fucci-Tg/Foxp3$^{hCD2/hCD52}$ mice on day 12 (Colitis). (**d**,**e**) dMLN (**d**) or proximal colon (**e**) of DSS-treated and control KikGR/Foxp3$^{hCD2/hCD52}$ mice on day 12 (Colitis) were photoconverted and flow cytometric analysis was performed 24 h later. The proportions of photoconverted CD25$^{+/-}$and CD25^{++} Tregs in indicated tissues are shown. These flow cytometry data are representative of at least two independent experiments; values in the plots indicate the percentage of the parent population. Data in bar graphs represent means ± s.e.m. ($n = 5$–8). Statistical comparisons were performed using Mann–Whitney's *U*-test (*$p < 0.05$).

LAG3, and CTLA-4, (but not CD103 and PD-1) expression was upregulated in CD25$^{+/-}$ Tregs in animals with colitis compared with total Tregs (which were largely CD25$^{+/-}$ Tregs (**Figure 7a**)) in untreated mice. Furthermore, CD25^{++} Tregs induced in colitis expressed the highest levels of ICOS, LAG3, CTLA-4, CD103 and PD-1 compared to other Treg subsets. We also detected an increase in CTLA-4 expression in migratory Tregs compared to Tregs pre-existing within the draining LN for both CD25^{++} and CD25$^{+/-}$ Tregs (**Figure 8b** and **Supplementary Figure S12**).

Notably, the proportions of photoconverted and non-photoconverted Nrp-1^{-} pTregs increased in dMLN in animals with colitis compared with those in untreated mice, suggesting that LN pTregs were augmented to a greater than tTregs during colon inflammation. The proportion of pTregs among CD25^{++} Tregs was similar to that among CD25$^{+/-}$Tregs (**Supplementary Figure S11** and **S12b**). Taken together, our results indicate that the expression of immunosuppressive molecules was increased in both CD25^{++} and CD25$^{+/-}$ Treg subsets in the draining LN of animals with colitis. These results suggested that Tregs in dMLN display an immunosuppressive phenotype in colonic inflammation.

We next analyzed the expression of molecules involved in T-cell migration. Gut-homing integrin α4β7 (ref. 40), but not CXCR4 (ref. 41) was expressed more highly on migratory compared to lymph node Tregs, particularly on CD25^{++} subset of migratory Tregs (**Supplementary Figure S13**). Expression of integrin α4β7 on lymph node CD25^{++} Tregs could indicate that these cells are poised to migrate to the inflamed colon. Furthermore, migratory CD25^{++} Tregs expressed more CCR5, which is upregulated after activation,[42] while expression of CCR7, a chemokine receptor involved in migration via high endothelial venues to LN,[43] was reduced on migratory Tregs. Taken together these results suggest that CD25^{++} Tregs received strong antigen stimulation and display a highly immunosuppressive colon-homing phenotype.

Next we analyzed the production of IL-10, an immunosuppressive cytokine important for inhibition of colitis, by photoconverted and non-photoconverted T cells in draining LN following photoconversion of the proximal colon. While, Tconvs expressed little IL-10 even after colitis induction, the frequency of IL-10 expressing cells was increased in Tregs in dMLN. Furthermore, photoconverted migratory Tregs in dMLN expressed significantly higher levels of IL-10 compared to non-photoconverted Tregs (60% vs. 35%) in colitis regardless of CD25 expression level (**Figure 8c**). These results suggested that colitis induces a large amount of IL-10 producing Tregs, especially among colonic migratory Tregs.

Finally, we tested colonic migratory Treg ability to inhibit effector T-cell proliferation *in vitro*. Twenty-four hours after

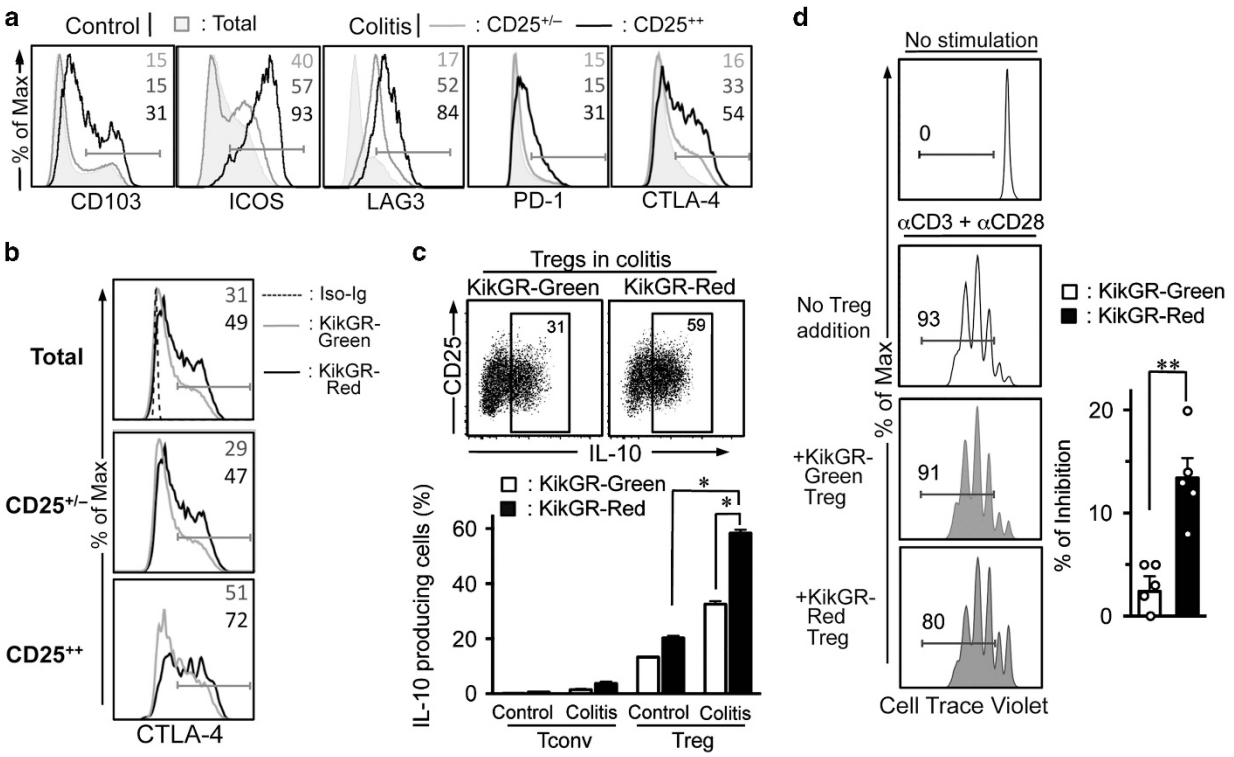

Figure 8 Colonic migratory Tregs in dMLN display superior immunosuppressive phenotype in colitis. Proximal colons of DSS-treated and control KikGR/Foxp3$^{hCD2/hCD52}$ mice were photoconverted on day 12 (Colitis) and flow cytometric analysis or cell sorting were performed 24 h later. CD103, ICOS, LAG3, PD-1, and CTLA-4 expression in total Tregs in control mice, CD25^{++} and CD25$^{+/-}$ Tregs in DSS-treated mice in dMLN (**a**), and CTLA-4 expression in CD25^{++} and CD25$^{+/-}$ photoconverted and non-photoconverted Tregs (**b**). These flow cytometry data are representative of at least four independent experiments. (**c**) The proportions of IL-10-producing cells out of photoconverted and non-photoconverted Tconvs and Tregs in dMLN stimulated with PMA/ionomycin and analyzed by flow cytometry; values in the plots indicate the percentage of the parent population. These data are representative of at least two independent experiments. Data in bar graphs are represented means ± s.e.m. ($n = 4$). Statistical comparisons were performed using Mann–Whitney's *U*-test (*$P < 0.05$). (**d**) CellTrace Violet-labeled CD4$^+$CD25$^-$ cells were co-cultured for 72 h with sorted photoconverted and non-photoconverted Tregs from dMLN of DSS-treated mice on day 12 (in the ratio of 1 Treg to 4 CD4$^+$CD25$^-$ cells) with or without stimulation with anti-CD3ε and anti-CD28 antibodies. Fluorescent intensity of CellTrace Violet-labeled CD4$^+$CD25$^-$ cells was measured by flow cytometry. These data are representative of five independent experiments; values in the histogram plots indicate the percentage of the parent population. The graph shows percentage inhibition relative to "No added Treg" group. Each symbol represents an individual replicate. Data in bar graph are represented means ± s.e.m. (n = 5). Statistical comparisons were performed using Mann–Whitney's *U*-test (**$P < 0.01$, *$P < 0.05$).

photoconversion of the proximal colon, photoconverted and non-photoconverted Tregs were purified from draining LN and mixed with CellTrace Violet-labeled CD4$^+$CD25$^-$ cells undergoing anti-CD3ε/CD28 stimulation (**Figure 8d**). In this setting photoconverted Tregs inhibited T-cell proliferation to a greater extent than non-photoconverted Tregs. These results suggest that colonic migratory Tregs possess a highly immunosuppressive phenotype and are, therefore, likely to control colonic immune responses in draining LN.

DISCUSSION

The identity of Treg subsets that regulate colitis remains poorly defined. We therefore elucidated the phenotype and dynamics of Tregs that emigrate from the caecum and ascending colon in the steady state and during colitis. Using Prox1-GFP mice to visualize afferent lymph vessels and KikGR mice to track immune cell migration, we identified dMLN as the exclusive draining site for the caecum and ascending colon. This result is consistent with a much earlier study that demonstrated that dMLN was the draining region for dye injected subserosally into the same regions of intestinal tract.[26] Likewise, analysis of cell migration from distinct regions of intestinal tract to draining LN showed that, cells in transverse colon migrate to colic LN,[29] and those in descending colon migrate to caudal LN.[24] Thus, our results refine our understanding of the lymphatic drainage network and migratory pathways that link the colon to draining LN.

While dMLN and mMLN are anatomically linked, it is likely that lymph flow through dMLN and mMLN is separate. In addition, immune cell egress from dMLN occurs either outside of mMLN or without cell retention within mMLN, since we did not detect any evidence of an immune response (such as T-cell proliferation or LN enlargement) in mMLN in animals with colitis. Furthermore, we have previously demonstrated that when two LNs are directly connected by a lymphatic vessel, the majority of photoconverted cells were observed in the downstream LN after photoconversion of an upstream LN,[23] however, no such influx of photoconverted cells was detected in mMLN after photoconversion of dMLN (data not shown).

We found that in the steady state, Tregs that arrived in the draining LN from the colon expressed higher level of inhibitory molecules ICOS and LAG3. Interestingly, ICOS expression in $CD25^{+}$ Treg was higher than $CD25^{lo/-}$ Tregs in both photoconverted and non-photoconverted populations. CD25 is upregulated after TCR stimulation. Thus, it is likely that $CD25^{+}$ Tregs received TCR signaling and were activated leading to higher expression of immunosuppressive molecules compared with $CD25^{lo/-}$ cells.

Compared to the steady state, colitis caused a marked upregulation of ICOS, LAG3, and CTLA-4 expression in $CD25^{++}$ and a modest increase in expression in $CD25^{+/-}$ Tregs in dMLN. Upregulation of these molecules was observed both in photoconverted and non-photoconverted Tregs. These results suggest that both colonic migratory and pre-existing LN Tregs in dMLN possess immunosuppressive properties in colonic inflammation. Furthermore, Tregs that arrived in draining LN from the inflamed colon expressed higher levels of ICOS, PD-1, CTLA-4, and IL-10 and inhibited T-cell proliferation to a greater extent than pre-existing LN Tregs. Thus, Tregs with superior immunosuppressive features are induced during the recovery phase of colitis and recirculate between proximal colon and dMLN. We hypothesize that these Tregs may play an important role in the downregulation of inflammatory responses in the colon. In addition to $Foxp3^{+}$ Tregs, $CD4^{+}Foxp3^{-}$ IL-10^{+} Tr1 cells are known to exist mainly in mucosal region and regulate colonic immune system and contribute to the cure of colitis.[44,45] However, given that we detected only small numbers of $CD4^{+}Foxp3^{-}$ IL-10^{+} cells in draining LN compared with $Foxp3^{+}$ Tregs, it is likely that $Foxp3^{+}$ Tregs rather than Tr1 cells facilitate recovery from colitis in the draining LN in DSS-induced colitis model.

We found that colitis induced vigorous proliferation of $CD25^{++}$ T cells in dMLN and also unexpectedly in the colon. Clostridia strains and other commensal bacteria strains, such as *Bacteroide fragilis* are able to generate and maintain Tregs.[15,16] Thus, it's possible that $CD25^{++}$ T-cell proliferation in the draining LN and inflamed colon is driven by bacterial antigens. Human Tregs expressing high levels of CD25 are defined as activated Tregs.[1] Furthermore, $CD25^{++}$ Tregs are generated in contact hypersensitivity response.[25] Given that activated $CD25^{++}$ Tregs with superior immunosuppressive capacity were generated in both draining LN and inflamed tissues and migrated bidirectionally between draining LN and inflamed tissues, this Treg subset may be involved in mediating immune suppression in both locations. Furthermore, this inhibitory mechanism could play a role in the recovery phase of the immune response and in maintenance of homeostasis. However, further investigations are needed to define the precise role of $CD25^{++}$ Tregs in this context.

We used FTY720 to demonstrate that S1P-S1PR1 signaling plays a critical role in egress of Tregs and all other T-cell subsets from the proximal colon in the steady state. FTY-720 treatment ameliorates DSS-induced colitis by sequestering T cells in secondary lymphoid tissues, leading to a drop in recirculating T cells and inhibition of T-cell migration to the inflamed colon.[46] However, our data suggests that FTY-720-mediated Treg retention in the colon is an additional mechanism for amelioration of DSS-induced colitis.

During the recovery phase of colitis, bidirectional $CD25^{++}$ and $CD25^{+/-}$ Treg migration between the colon and draining LN and Treg replacement in the colon were accelerated. While the expression of CCR7 was decreased in all Treg subsets in dMLN, we showed that $CD25^{++}$ (and to a lesser extent $CD25^{+/-}$) Tregs expressed a high level of α4β7 integrin. Notably, one of the ligands of integrin α4β7, Mucosal addressin Cell Adhesion Molecule-1 (MadCAM-1), is expressed in vessels in colonic LP and is important for gut homing.[47] Furthermore, MadCAM-1 expression is upregulated in patients with diseases of the colon and in experimental animal models including DSS-induced colitis.[48,49] Thus, our results suggest that enhancement of integrin α4β7 interaction with MadCAM-1 may play a role in enhancing Treg migration in colitis. Taken together, these molecular changes in Tregs and gut tissue induced by colitis facilitate a significant increase in migration from draining LN to inflamed colon and inflamed colon-trophic Treg migration.

Recently, regulation of immune diseases via inhibition of immune cell migration has been the focus of intensive research. For instance, anti-integrin α4β7 antibody (Vedolizumab) has been used for inhibition of effector T-cell migration to colitis sites, and shown to be effective in treatment of moderate to severe ulcerative colitis in Phase III clinical trial (GEMINI study).[50] However, this treatment was ineffective in about half of patients. Our finding that Tregs, particularly $CD25^{++}$ Tregs with a superior immunosuppressive phenotype express high levels of integrin α4β7 and therefore may also be targeted by Vedolizumab highlights the importance of understanding Treg migration and function after Vedolizumab treatment in non-responsive patients.

In this study, we elucidated cellular dynamics and immunosuppressive features of colonic migratory Tregs during inflammation and homeostasis. An improved understanding of immunological features and migration between inflamed tissues, draining LN and other lymphoid organs will lead to enhanced correlation of local immune responses with systemic immune diseases.

METHODS

Mice. Prox1-GFP Tg mice were kindly provided by Dr Young-Kwon Hong.[28] Knock-in mice carrying KikGR cDNA under the CAG promoter (KikGR mice) were made previously.[23] FucciG_1-#639 and FucciS/G_2/M-#474 mice on BDF1 background were generated as described previously,[39] and were backcrossed to C57BL/6J mice (CREA Japan) more than ten times. The resulting progeny were crossed to prepare FucciG_1-#639/FucciS/G_2/M-#474 double transgenic mice (Fucci-Tg). $Foxp3^{hCD2/hCD52}$ mice were kindly provided by Dr. Shohei Hori.[30] KikGR mice or Fucci-Tg mice were intercrossed with $Foxp3^{hCD2/hCD52}$ mice to generate KikGR/$Foxp3^{hCD2/hCD52}$ mice or Fucci-Tg/$Foxp3^{hCD2/hCD52}$ mice and used in this study. These mice were bred in specific pathogen-free facilities at Kyoto University or Osaka Ohtani University. All experimental procedures were approved by the Institutional Animal Care and Use Committee of Kyoto

University Faculty of Medicine and Osaka-Ohtani University Faculty of Pharmacy.

Photoconversion, lymphography, and surgical procedures. During photoconversion of the large intestine or small intestine, non-photoconverted regions were protected from light using aluminum foil, and the region of the intestine targeted for photoconversion was drawn out from the abdominal cavity, and exposed to violet light (435 nm, 100 mW cm^{-2}) for 1 minute from the front and behind following laparotomy. Following photoconversion the abdominal wall was closed with bulldog forceps. Similarly, LNs were photoconverted by exposure to violet light (435 nm, 100 mW cm^{-2}) for 2 min. This method ensured almost complete photoconversion of cells in LN.[22] To keep exposed tissues moist during exposure to light, warmed PBS was applied to the region of photoconversion. To prevent hypothermia, mice were kept warm by a heater during perioperative stages. Lymphography of mesentery was performed by local injection (27G) of 1% patent blue within the intestinal wall of the caecum, ascending colon, transverse colon, and ileum.

Bone-marrow-chimeric mice. Wild-type C57BL/6 mice or Prox1-GFP mice were lethally irradiated (9.25 Gy) and transferred with 1×10^7 bone marrow cells from KikGR/Foxp3$^{hCD2/hCD52}$ mice. Experiments were conducted at least 8 weeks following bone marrow cell transfer to allow for reconstitution of immune cells in peripheral tissues. At this stage, hematopoietic chimerism (determined as the proportion of lymph node B cells that expressed KikGR) exceeded 98%.

Microscopy and histological study. Observations of mesenteric lymph vessels were performed using a fluorescence stereoscopic microscope (MVX10, Olympus, Tokyo, Japan). Due to the strong KikGR signal from stromal cells in KikGR mice making it difficult to detect KikGR signal from hematopoietic cells, KikGR/Foxp3$^{hCD2/hCD52}$ bone marrow chimeric (KikGR-BM chimeric) mice were used to facilitate the visualization of KikGR by histological analysis. To observe KikGR migratory cells from proximal colons in MLN, proximal colons of KikGR-BM chimeric mice were photoconverted. Six hours after photoconversion, dMLN and ileocecal side of mMLN were dissected, fixed in 4% paraformaldehyde (Wako Chemicals, Osaka, Japan), and replaced with 30% sucrose as a cryoprotectant. Frozen tissue sections were prepared and observed using a confocal microscope (LSM-710, Carl Zeiss, Oberkochen, Germany).

Cell isolation from LNs and colons. Preparation of cell suspensions from LNs[22,23] and colons[51] were described previously. Briefly, resected colons were washed in PBS, stirred in 1 μM EDTA buffer (pH 8.0) at 37 °C, and minced with scissors. The minced tissue was stirred for 80 min at 37 °C in collagenase (1.5 mg ml^{-1}; Wako, Osaka, Japan) and dispase (1 U ml^{-1}; BD Bioscience) containing RPMI-1640 medium. Cell suspensions were filtered with 40 μm cell strainer.

Antibodies and flow cytometry. Fluorochrome-conjugated or biotinylated antibodies and fluorochrome-conjugated avidin were obtained from BD Bioscience (Franklin Lakes, NJ), eBioscience (San Diego, CA), or BioLegends (San Diego, CA). Details are listed in **Supplementary Table S1**. For flow cytometric analysis, cells were washed with Dulbecco's PBS containing 2% FCS and 0.02% sodium azide. Next, cells were incubated with 2.4G2 hybridoma culture supernatant to block Fc binding, then stained with biotinylated mAbs followed by Brilliant Violet 421 or Allophycocyanin (APC)-conjugated streptavidin or fluorochrome-labeled mAbs for 15 min at 4 °C. Dead cells were labeled with 7-amino-actinomycin D (BioLegend) or propidium iodide. For intracelleur staining, the cells were fixed, permeabilized, and stained with BV421-conjugated anti-CTLA-4. For intracellular staining for IL-10, monensin (BD Bioscience) was added to the culture stimulated with PMA/ionomycin for 4 h. The cells were then fixed, permeabilized, and stained with APC-conjugated anti-IL-10 antibody. Stained samples were acquired using Fortessa (BD Bioscience) or SP6800 (SONY, Tokyo, Japan). Using Fortessa, KikGR green and red signals were detected using 530/60 and 595/50 bandpass filters, respectively. Flow cytometry data were analyzed using Flowjo software (Tree Star, Ashland, OR).

Inhibition of T cell egress from colon. Photoconversion of proximal colon was performed 30 min after FTY720 (Cayman Chemical, Ann Arbor, MI) administration (100 μg per mouse, i.p.). Twenty-four hours after photoconversion, the proximal colon and dMLN were resected, and stained samples were acquired using flow cytometry.

DSS-induced colitis model. To induce colitis 10–12-week-old male mice (body weight >25 g) were given 3% DSS (Wako) solution in drinking water for 7 days, and then water alone. Body weight was measured every 16 days. Colon length was measured as resected whole colon.

Effector T-cell proliferation inhibition assay. LN cell suspensions from Foxp3$^{hCD2/hCD52}$ mice (pool of 6–8 mice) were stained with APC-conjugated anti-hCD2 antibody and APC-positive cells were positively selected using anti-APC magnetic microbeads (Miltenyi Biotec, Bergisch Gladbach, Germany). Sorted cells were stained with APC-Alexa750-conjugated anti-mouse CD4 antibody, and CD4$^+$ hCD2$^+$ KikGR-Red and KikGR-Green populations were sorted by SH800 (SONY). Splenocytes were stained with biotinylated-CD8, CD11b, CD11c, CD19, CD25, CD49b, and TER-119 mAb and CD4$^+$CD25$^-$ cells were negatively sorted using anti-biotin MACS beads (Miltenyi Biotec). Purity of CD4$^+$CD25$^-$ cells was $>95\%$. CD4$^+$CD25$^-$ cells (5.0×10^4 cells) were labeled with CellTrace Violet (Thermo Scientific, Waltham, MA) and co-cultured with sorted Tregs (1.25×10^4 cells) for 72 h in αCD3ε-coated (2 μg ml^{-1}) 96-well plate with anti-CD28 antibody (2 μg ml^{-1}) in 2-ME containing RPMI-1640 medium. After 3 days of culture, cells were harvested and stained with PI, APC-Cy7-conjugated anti-CD4 antibody, and Alexa647-conjugated anti-CD5 antibody and analyzed by flow cytometry. Inhibition of effector T-cell proliferation was evaluated by dilution of CellTrace Violet.

Statistical analysis. Mann–Whitney's *U*-test was performed using GraphPad Prism version 6.0 (GraphPad Software, San Diego, CA). Data in bar graphs represent means ± s.e.m. *P*-values of <0.05 were considered to be statistically significant.

SUPPLEMENTARY MATERIAL is linked to the online version of the paper at http://www.nature.com/mi

ACKNOWLEDGMENTS

This work was supported in part by JSPS Grants-in-Aid for Scientific Research in Innovative Areas "Analysis and Synthesis of Multidimensional Immune Organ Network" (#24111007); JSPS Grants-in-Aid for Scientific Research (B) (#16H05087); Special Coordination Funds for Promoting Science and Technology of the Japanese Government; National Health and Medical Research Council Australia project grants GNT1062328 and 1062332 (T.C.) and Astellas Pharma Inc. through the Formation of Innovation Centers for the Fusion of Advanced Technologies Program. Foxp3$^{hCD2/hCD52}$ mice provided by Dr. Shohei Hori from the RIKEN Research Center and Prox1-GFP mice provided by Dr. Young-Kwon Hong were of great assistance in this study.

AUTHOR CONTRIBUTIONS

Y.N., R.I, Y.K., O.H., Y.S. and M.T. designed experiments. Y.N. and R.I. performed experiments. T.H. and K.K. prepared Prox1-GFP mice. Y.N., R.I., and M.T. analyzed the data. Y.N., T.C., T.W., Y.S. and M.T. wrote the manuscript.

DISCLOSURE

The authors declared no conflict of interest.

REFERENCES

1. Sakaguchi, S., Yamaguchi, T., Nomura, T. & Ono, M. Regulatory T cells and immune tolerance. *Cell* **133**, 775–787 (2008).
2. Lu, L. & Rudensky, A. Regulatory T cells: mechanisms of differentiation and function. *Annu. Rev. Immunol.* **30**, 531 (2012).
3. Bennett, C.L. *et al.* The immune dysregulation, polyendocrinopathy, enteropathy, X-linked syndrome (IPEX) is caused by mutations of FOXP3. *Nat. Genet.* **27**, 20–21 (2001).
4. Wildin, R.S. *et al.* X-linked neonatal diabetes mellitus, enteropathy and endocrinopathy syndrome is the human equivalent of mouse scurfy. *Nat. Genet.* **27**, 18–20 (2001).
5. Maul, J. *et al.* Peripheral and intestinal regulatory $CD4^+CD25^{high}$ T cells in inflammatory bowel disease. *Gastroenterology* **128**, 1868–1878 (2005).
6. Makita, S. *et al.* $CD4^+CD25^{bright}$ T cells in human intestinal lamina propria as regulatory cells. *J. Immunol.* **173**, 3119–3130 (2004).
7. Chaudhry, A. *et al.* Interleukin-10 signaling in regulatory T cell is required for suppression of TH17 cell-mediated inflammation. *Immunity* **34**, 566–578 (2011).
8. Fantini, M.C. *et al.* Transforming growth factor beta induced $FoxP3^+$ regulatory T cells suppress Th1 mediated experimental colitis. *Gut* **55**, 671–680 (2006).
9. Rubtsov, Y.P. *et al.* Regulatory T cell-derived interleukin-10 limits inflammation at environmental interfaces. *Immunity* **28**, 546–558 (2008).
10. Tomoki, I. *et al.* Two functional subsets of $Foxp3^+$ regulatory T cells in human thymus and periphery. *Immunity* **28**, 870–880 (2008).
11. Liu, H., Hu, B., Xu, D. & Liew, F.Y. $CD4^+CD25^+$ regulatory T cells cure murine colitis: the role of IL-10, TGF-beta, and CTLA4. *J. Immunol.* **171**, 5012–5017 (2003).
12. Do, J. *et al.* An IL-27/Lag3 axis enhances $Foxp3^+$ regulatory T cell–suppressive function and therapeutic efficacy. *Mucosal Immunol.* **9**, 1–9 (2015).
13. Francisco, L.M., Sage, P.T. & Sharpe, A.H. PD-1 pathway in tolerance and autoimmunity. *Immunol. Rev.* **236**, 219–242 (2010).
14. Pedros, C., Duguet, F., Saoudi, A. & Chabod, M. Disrupted regulatory T cell homeostasis in inflammatory bowel diseases. *World J. Gastroenterol.* **22**, 974–995 (2016).
15. Tanoue, T., Atarashi, K. & Honda, K. Development and maintenance of intestinal regulatory T cells. *Nat. Rev. Immunol.* **16**, 295–309 (2016).
16. Round, J.L. & Mazmanian, S.K. Inducible $Foxp3^+$ regulatory T-cell development by a commensal bacterium of the intestinal microbiota. *Proc. Natl Acad. Sci. USA* **107**, 12204–12209 (2010).
17. Hayashi, H., Takahashi, R., Nishi, T., Sakamoto, M. & Benno, Y. Molecular analysis of jejunal, ileal, caecal and rectosigmoidal human colonic microbiota using 16S rRNA gene libraries and terminal restriction fragment length polymorphism. *J. Med. Microbiol.* **54**, 1093–1101 (2005).
18. Wolff, M.J. *et al.* TH17, TH22 and TReg cells are enriched in the healthy human cecum. *PLoS ONE* **7**, e41373 (2012).
19. Atarashi, K. *et al.* Induction of colonic regulatory T cells by indigenous Clostridium species. *Science* **48**, 1–6 (2010).
20. Ando, R., Hama, H., Yamamoto-Hino, M., Mizuno, H. & Miyawaki, A. An optical marker based on the UV-induced green-to-red photoconversion of a fluorescent protein. *Proc. Natl Acad. Sci. USA* **99**, 12651–12656 (2002).
21. Tsutsui, H., Karasawa, S., Shimizu, H., Nukina, N. & Miyawaki, A. Semi-rational engineering of a coral fluorescent protein into an efficient highlighter. *EMBO Rep.* **6**, 233–238 (2005).
22. Tomura, M. *et al.* Monitoring cellular movement *in vivo* with photoconvertible fluorescence protein 'Kaede' transgenic mice. *Proc. Natl Acad. Sci. USA* **105**, 10871–10876 (2008).
23. Tomura, M. *et al.* Tracking and quantification of dendritic cell migration and antigen trafficking between the skin and lymph nodes. *Sci. Rep.* **4**, e6030 (2014).
24. Morton, A.M. *et al.* Endoscopic photoconversion reveals unexpectedly broad leukocyte trafficking to and from the gut. *Proc. Natl Acad. Sci. USA* **111**, 6696–6701 (2014).
25. Tomura, M. *et al.* Activated regulatory T cells are the major T cell type emigrating from the skin during a cutaneous immune response in mice. *J. Clin. Invest.* **120**, 883–893 (2010).
26. Carter, P.B. & Collins, F.M. The route of enteric infection in normal mice. *J. Exp. Med.* **139**, 1189–1203 (1974).
27. Houston, S.A. *et al.* The lymph nodes draining the small intestine and colon are anatomically separate and immunologically distinct. *Mucosal Immunol.* **9**, 468–478 (2015).
28. Choi, I. *et al.* Visualization of lymphatic vessels by Prox1-promoter directed GFP reporter in a bacterial artificial chromosome-based transgenic mouse. *Blood* **117**, 362–365 (2011).
29. Van den Broeck, W., Derore, A. & Simoens, P. Anatomy and nomenclature of murine lymph nodes: descriptive study and nomenclatory standardization in BALB/cAnNCrl mice. *J. Immunol. Methods* **312**, 12–19 (2006).
30. Komatsu, N. *et al.* Heterogeneity of natural $Foxp3^+$ T cells: a committed regulatory T-cell lineage and an uncommitted minor population retaining plasticity. *Proc. Natl Acad. Sci. USA* **106**, 1903–1908 (2009).
31. Laffont, S., Siddiqui, K.R.R. & Powrie, F. Intestinal inflammation abrogates the tolerogenic properties of MLN $CD103^+$ dendritic cells. *Eur. J. Immunol.* **40**, 1877–1883 (2010).
32. Barnes, M.J. & Powrie, F. Regulatory T cells reinforce intestinal homeostasis. *Immunity* **31**, 401–411 (2009).
33. Pappu, R. *et al.* Promotion of lymphocyte egress into blood and lymph by distinct sources of sphingosine-1-phosphate. *Science* **316**, 295–298 (2007).
34. Tomura, M., Itoh, K. & Kanagawa, O. Naive $CD4^+$ T lymphocytes circulate through lymphoid organs to interact with endogenous antigens and upregulate their function. *J. Immunol.* **184**, 4646–4653 (2010).
35. Ledgerwood, L.G. *et al.* The sphingosine 1-phosphate receptor 1 causes tissue retention by inhibiting the entry of peripheral tissue T lymphocytes into afferent lymphatics. *Nat. Immunol.* **9**, 42–53 (2008).
36. Bromley, S.K., Yan, S., Tomura, M., Kanagawa, O. & Luster, A.D. Recirculating memory T cells are a unique subset of $CD4^+$ T cells with a distinct phenotype and migratory pattern. *J. Immunol.* **190**, 970–976 (2013).
37. Weiss, J.M. *et al.* Neuropilin 1 is expressed on thymus-derived natural regulatory T cells, but not mucosa-generated induced $Foxp3^+$ Treg cells. *J. Exp. Med.* **209**, 1723–1742 (2012).
38. Yu, Q.T. *et al.* Expression and functional characterization of $FOXP3^+$ $CD4^+$ regulatory T cells in ulcerative colitis. *Inflamm. Bowel Dis.* **13**, 191–199 (2007).
39. Tomura, M. *et al.* Contrasting quiescent G_0 phase with mitotic cell cycling in the mouse immune system. *PLoS ONE* **8**, e73801 (2013).
40. Schweighoffer, T. *et al.* Selective expression of integrin alpha-4-beta-7 on a subset of human CD4(+) memory T-cells with hallmarks of gut-trophism. *J. Immunol.* **151**, 717–729 (1993).
41. Mikami, S. *et al.* Blockade of CXCL12/CXCR4 axis ameliorates murine experimental colitis. *Pharmacol. Res. Perspect.* **327**, 383–392 (2008).
42. Kang, S.G. *et al.* Identification of a chemokine network that recruits $FoxP3^+$ regulatory T cells into chronically inflamed intestine. *Gastroenterology* **132**, 966–981 (2007).
43. Campbell, J.J. *et al.* 6-C-kine (SLC), a lymphocyte adhesion-triggering chemokine expressed by high endothelium, is an agonist for the MIP-3β receptor CCR7. *J. Cell Biol.* **141**, 1053–1059 (1998).
44. Groux, H. *et al.* A $CD4^+$ T-cell subset inhibits antigen-specific T-cell responses and prevents colitis. *Nature* **389**, 737–742 (1997).
45. Izcue, A., Coombes, J.L. & Powrie, F. Regulatory lymphocytes and intestinal inflammation. *Annu. Rev. Immunol.* **267**, 313–338 (2009).
46. Deguchi, Y. *et al.* The S1P receptor modulator FTY720 prevents the development of experimental colitis in mice. *Oncol. Rep.* **16**, 699–703 (2006).
47. Berlin, C. *et al.* Alpha 4 beta 7 integrin mediates lymphocyte binding to the mucosal vascular addressin MAdCAM-1. *Cell* **74**, 185–195 (1993).
48. Briskin, M. *et al.* Human mucosal addressin cell adhesion molecule-1 is preferentially expressed in intestinal tract and associated lymphoid tissue. *Am. J. Pathol.* **151**, 97–110 (1997).
49. Kato, S. *et al.* Amelioration of murine experimental colitis by inhibition of mucosal addressin cell adhesion molecule-1. *Pharmacol. Res. Perspect.* **295**, 183–189 (2000).
50. Feagan, B.G. *et al.* Vedolizumab as induction and maintenance therapy for ulcerative colitis. *N. Engl. J. Med.* **369**, 699–710 (2013).
51. Ha, S. *et al.* Regulation of B1 cell migration by signals through Toll-like receptors. *J. Exp. Med.* **203**, 2541–2550 (2006).